Title

Tapes, Sheets, and Prisms. Identification of the Weak C−F Interactions that Steer Fullerene−Porphyrin Cocrystallization

Journal

Crystal Growth & Design, 6(2)

ISSN

1528-7483

Authors

Hosseini, Ali
Hodgson, Michael C
Tham, Fook S
et al.

Publication Date

2006-02-01

DOI

10.1021/cg050352n

Peer reviewed

CRYSTAL GROWTH & DESIGN
2006
VOL. 6, NO. 2
397−403

Tapes, Sheets, and Prisms. Identification of the Weak C−F Interactions that Steer Fullerene−Porphyrin Cocrystallization

Ali Hosseini,[†] Michael C. Hodgson,[†] Fook S. Tham,[§] Christopher A. Reed,[§] and Peter D. W. Boyd*,[†]

Department of Chemistry, The University of Auckland, Private Bag 92019, Auckland, New Zealand, and Department of Chemistry, University of California, Riverside, California 92521

Received July 20, 2005; Revised Manuscript Received September 25, 2005

ABSTRACT: Tetra(pentafluorophenyl)porphyrin (H_2TPFPP) has been cocrystallized with C_{60} from arene solvents to give H_2TPFPP·C_{60}, **1**, H_2TPFPP·C_{60}·8Benzene, **3**, and 3H_2TPFPP·2C_{60}·6Toluene, **4**. Their X-ray structures have been determined to identify the supramolecular interactions that lead to tape, sheet, and prismatic packing motifs. In addition to close fullerene−porphyrin $\pi-\pi$ interactions, attractive C−F···H−C interactions are important in connecting the C_6F_5 groups of one porphyrin to the pyrrole positions of a neighbor. This interaction is also seen in the structure of the free-base porphyrin H_2TPFPP·3*p*-Xylene, **2**.

Introduction

Fullerenes and porphyrins are spontaneously attracted to each other.[1] This new supramolecular recognition element is the basis of a rapidly growing class of fullerene-porphyrin cocrystallates which contain a variety of tape, sheet and 3D structural motifs.[2−8] To date, little attention has been paid to the additional crystal forces that augment the fullerene-porphyrin interaction and which ultimately determine the particular motif that is observed. In all structures determined so far, a fullerene is centered over a porphyrin (or metalloporphyrin) with unusually close atom-to-atom approaches and this appears to be a major structure-determining element. For example, when fullerenes are intercalated between tapes and sheets of metal-linked tetra-*p*-pyridylporphyrins, the tapes and sheets are brought from a slipped configuration into strict tetragonal register.[4] In less sterically hindered octaethylporphyrins, face-to-face porphyrin interactions are common and in the absence of steric effects, the hierarchy of interaction strengths is clearly porphyrin/porphyrin > porphyrin/fullerene > fullerene/fullerene. In tetraphenylporphyrin cocrystallizations, weak *ortho*-C−H···$\pi_{\text{fullerene}}$ interactions augment the $\pi-\pi$ interaction[2] and DFT calculations suggest these may account for as much as 20% of the interaction strength when four C−H bonds are involved.[9]

In this paper, we report three cocrystallizations of pentafluorophenyl-substituted porphyrins with C_{60}. These fluorinated porphyrins, in addition to the expected fullerene-porphyrin $\pi-\pi$ interaction, have a number of intermolecular interactions involving C−F bonds. The 1997 observation that C−F bonds "...hardly ever accept hydrogen bonds..."[10] might lead to the expectation that C−F bonds would be relatively unimportant in dictating lattice structure but it is now apparent that several structure-defining C−F bond interactions can be identified in the crystal structures of fluoro compounds.[11] Some of these can be identified in the fluoroporphyrin/fullerene cocrystallates isolated in the present work and they provide an opportunity to map the interactions that lead to their tape, sheet and prism lattice motifs. A preliminary report on one of the present structures,[1] suggested that an attractive C−F···H−C interaction was important in connecting the C_6F_5 groups of one porphyrin to the pyrrole positions of a neighbor. After submission of this work, a report on the structures of four other fluoroporphyrin/fullerene cocrystallizations appeared.[12]

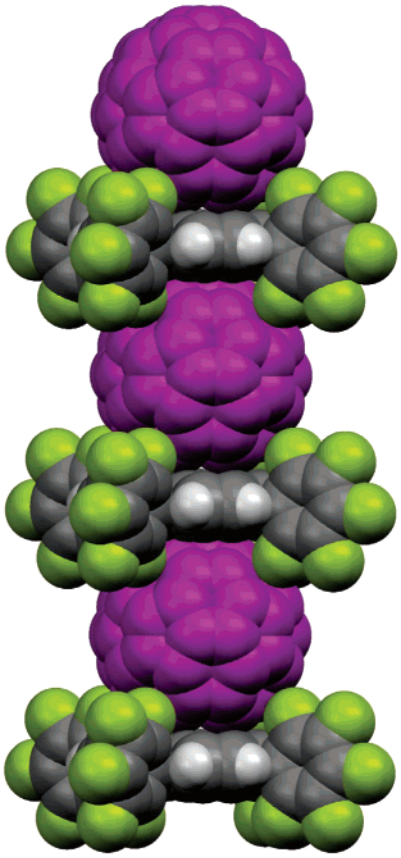

Figure 1. Space-filling model of linear alternating fullerene−porphyrin columns in H_2TPFPP·C_{60}, **1**.

Experimental Section

Tetra(pentafluorophenyl)porphyrin (H_2TPFPP) was prepared by dropwise addition of freshly distilled pyrrole to a hot solution of pentafluorobenzaldehyde in propionic acid followed by reflux for 1 h.[13] Crystals isolated on cooling were purified by column chromatography (silica gel/CH_2Cl_2 eluent). C_{60} was purchased from MER (Tucson, AZ). Solvents (HPLC grade) were used as supplied. Crystallizations

* To whom correspondence should be addressed. E-mail: pdw.boyd@auckland.ac.nz.
[†] The University of Auckland.
[§] University of California, Riverside.

10.1021/cg050352n CCC: $33.50
Published on Web 11/03/2005

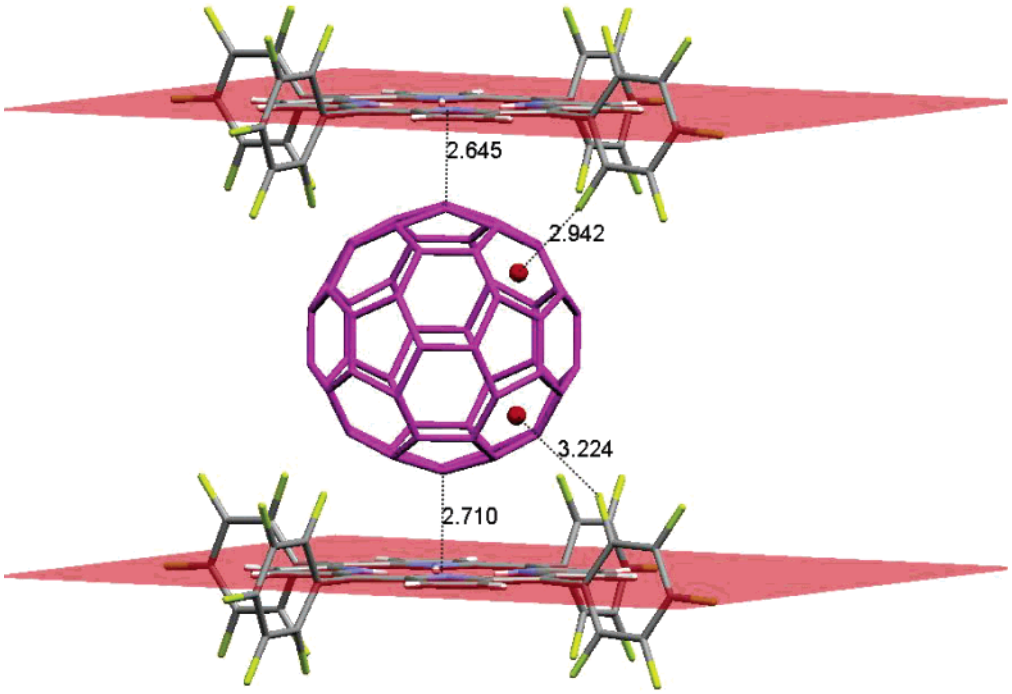

Figure 2. Close approach of C_{60} (one 50% occupied site) to the 24-atom mean plane of the porphyrin, and *ortho* F atoms to the centers of the fullerene six-membered rings in $H_2TPFPP{\cdot}C_{60}$, **1**.

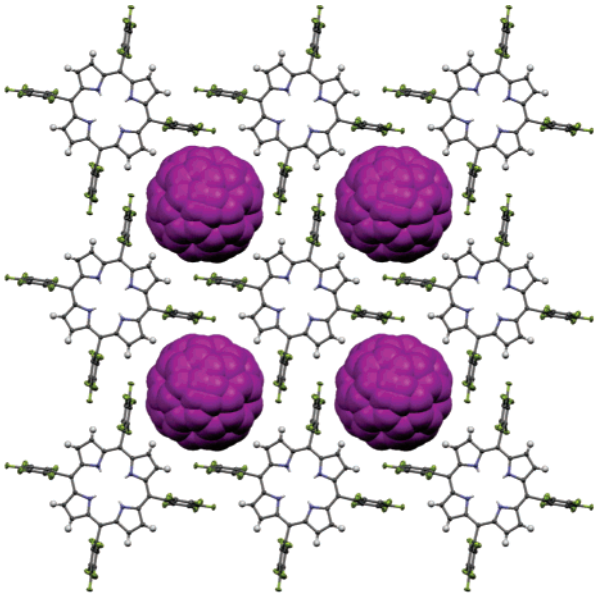

Figure 3. Tetragonal sheet of H_2TPFPP formed by *p*-phenyl C−F···H−C porphyrin interactions in $H_2TPFPP{\cdot}C_{60}$, **1**, viewed along the *c* axis with space-filling model for disordered C_{60} and thermal ellipsoids (50% probability) for the 91.1% occupied site of H_2TPFPP.

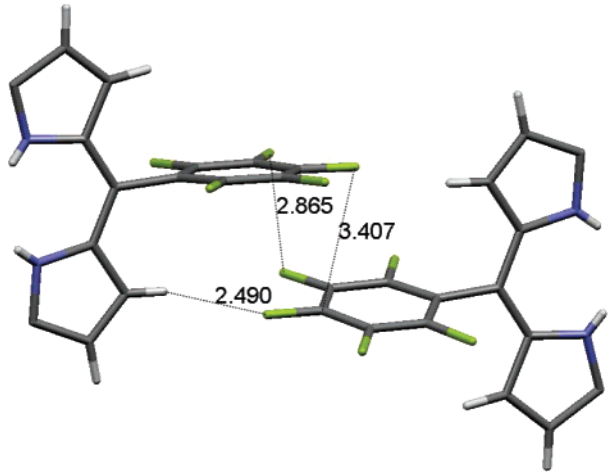

Figure 4. Porphyrin F···H and F···C contacts in $H_2TPFPP{\cdot}C_{60}$, **1**.

were performed by slow evaporation at room temperature of 1:1 solutions of H_2TPFPP and C_{60}. From benzene and toluene respectively, fullerene/porphyrin cocrystallates **3** and **4** were formed. From *p*-xylene, brown crystals of **2** incorporating no C_{60} in the lattice were formed. However, redissolution of **2** by gentle heating of the original mother liquor containing a higher concentration of C_{60}, followed by slow cooling, gave two types of crystal, the original brown material and red crystals of the fullerene/porphyrin *p*-xylene solvate **1**. Crystals of **1** were also obtained from toluene/dichloromethane mixtures.

Intensity data (λ_{Mo} = 0.71073 Å) for **1**−**3** were collected on a Siemens SMART diffractometer at The University of Auckland and for **4** at the University of California Riverside on a Bruker APEX2 platform-CCD X-ray diffractometer system. Absorption corrections were applied to the raw intensity data using the SADABS program[14] for structures **1**, **3** and **4** and XABS[15] for structure **2**. Structures were solved by direct methods using WINGX[16] with SHELXS-97[17] for structures **1** and **3** and SIR92[18] for structure **2**. The Bruker SHELXTL software package (version 6.14) was used for structure **4**.[19] Structures were refined using SHELXL-97. The crystal data and structural refinement details are given below and in the Supporting Information. Figures were created using The Cambridge Crystallographic Database Mercury visualization software.[20] For clarity, only one site is shown in structures containing disordered porphyrins or fullerenes, unless otherwise indicated.

$H_2TPFPP{\cdot}C_{60}$, 1. Red blocks, empirical formula, C_{104} H_{10} F_{20} N_4, fw 1695.16, T = 87 K, tetragonal, $P4/n$, a = 16.2344(2) Å, b = 16.2344(2) Å, c = 12.2612(2) Å, V = 3231.51(8) Å^3, Z = 2, D_c = 1.742 g/cm^3, μ = 0.143 mm^{-1}, $F(000)$ = 1684, crystal 0.42 × 0.30 × 0.16 mm^3, Θ_{max} = 25.97°, ranges $-13 \le h \le 14$, $0 \le k \le 19$, $0 \le l \le 14$, reflections collected = 18157, independent reflections = 3103, data/restraints/parameters 3103/570/473.

All non-hydrogen atoms were identified after isotropic refinement of the initial solution. The H-atoms were included in the refinement in calculated positions riding on the atoms to which they were attached. Full matrix least-squares refinement on F^2 with the constraint SIMU was carried out to give R indices [$I > 2\sigma(I)$], R1 = 0.0527, wR2 =

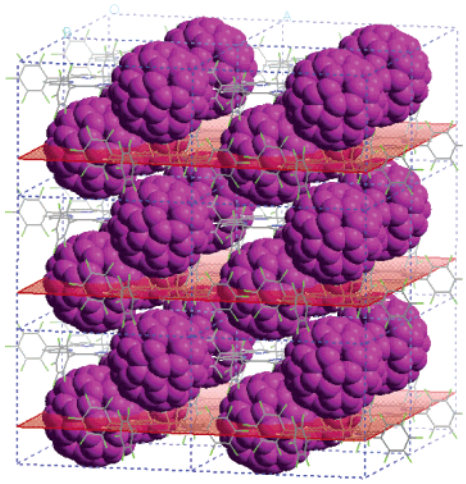

Figure 5. Alternating layered porphyrin sheets (stick model) separated by C_{60} molecules (space filling) in H_2TPFPP·C_{60}, **1**.

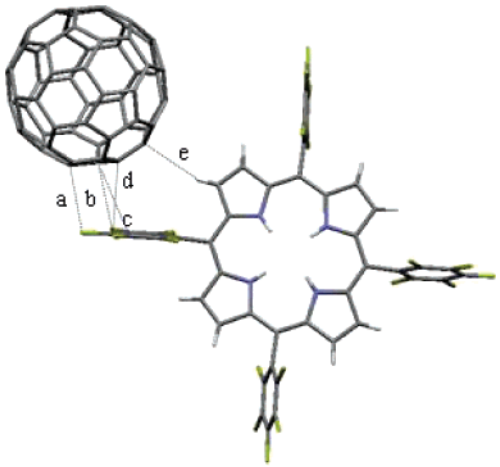

Figure 6. Fullerene interactions with surrounding porphyrin sheet in H_2TPFPP·C_{60}, **1**: contacts a = 3.03 Å, b = 3.30 Å, c = 3.36 Å, d = 3.22 Å, and e = 2.87 Å).

0.1431 and GOF = 1.085. There is disorder in the porphyrin molecule (site occupancy 91.1%/8.9%). The C_{60} has a 2-fold rotational disorder about the crystallographic 4-fold axis which passes through two 6:6 ring junctions at opposite ends of the molecule.

H_2TPFPP·3*p*-Xylene, 2. Brown needles, empirical formula, C_{34} H_{15} F_{10} N_2, fw 2565.92, T = 87 K, monoclinic, $P2_1/c$, a = 7.16440(10) Å, b = 24.8612(4) Å, c = 16.7746(3) Å, α = 90°, β = 107.4010(10)°, γ = 90°, V = 2851.08(8) Å^3, Z = 4, D_c = 1.494 g/cm^3, μ = 0.134 mm^{-1}, F(000) = 1292, crystal 0.28 × 0.2 × 0.14 mm^3, Θ_{max} = 26.09°, ranges −13 ≤ h ≤ 14, 0 ≤ k ≤ 19, 0 ≤ l ≤ 14, reflections collected = 22249, independent reflections = 5444, data/parameters 5444/455.

All non-hydrogen atoms were identified after isotropic refinement of the initial solution. Both *p*-xylene molecules are disordered (site occupancy ratios 50%/50%). The H-atoms were included in the refinement in calculated positions riding on the atoms to which they were attached for the porphyrin and the ordered xylene molecule. Full matrix least-squares refinement on F^2 was carried out to give R indices [$I > 2\sigma(I)$], R1 = 0.0820, wR2 = 0.2140 and GOF = 1.039.

H_2TPFPP·C_{60}·8Benzene, 3. Red blocks, empirical formula, C_{152} H_{56} F_{20} N_4, fw 2317.56, T = 87 K, tetragonal, $I4_1/a$, a = 28.7056(3) Å, b = 28.7056(3) Å, c = 12.39290(10)Å, α = 90°, β = 90°, γ = 90°, V = 10211.89(17Å^3, Z = 4, D_c = 1.507 g/cm^3, μ = 0.113 mm^{-1}, F(000) = 4703, crystal 0.36 × 0.2 × 0.12 mm^3, Θ_{max} = 25.37°, ranges −34 ≤ h ≤ 25, −24 ≤ k ≤ 34, −14 ≤ l ≤ 14, reflections collected = 17851, independent reflections = 4693, data/parameters 4693/438.

All non-hydrogen atoms were identified after isotropic refinement of the initial solution. The H-atoms were included in the refinement in calculated positions riding on the atoms to which they were attached.

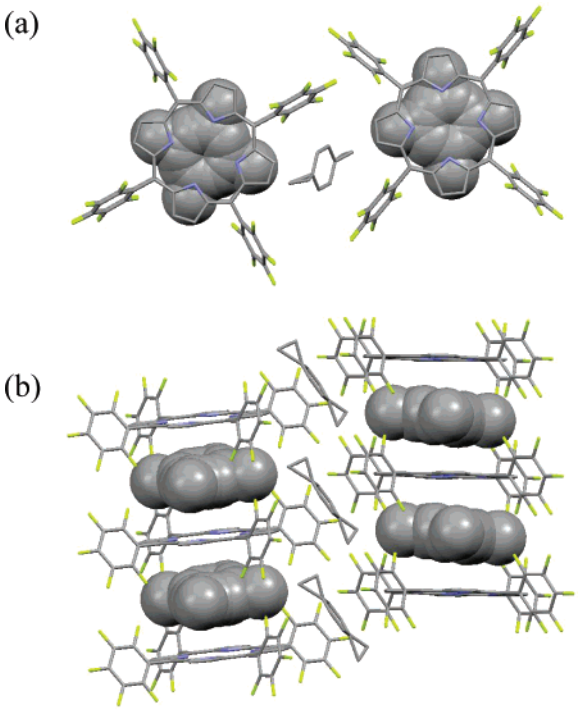

Figure 7. Views of the porphyrin stack in H_2TPFPP·3*p*-Xylene, **2**, showing disordered *p*-xylene sandwiched between porphyrins (space-filling model) and disordered *p*-xylene near phenyl groups (stick model): (a) viewed down the column axis; (b) orthogonal to the column axis.

Full matrix least-squares refinement on F^2 with constraints SIMU and DELU was carried out to give R indices [$I > 2\sigma(I)$], R1 = 0.0742, wR2 = 0.1178 and GOF = 1.053. As in structure **1**, the C_{60} has a 2-fold rotational disorder about the crystallographic 4-fold axis which passes through two 6:6 ring junctions at opposite ends of the molecule.

3H_2TPFPP·2C_{60}·6Toluene, 4. Black prisms, empirical formula, C_{168} H_{63} F_{30} N_6, fw 2735.24, T = 100 K, trigonal, $P\bar{3}$, a = 20.9965(4) Å, b = 20.9965(4) Å, c = 14.7377(6) Å, α = 90°, β = 90°, γ = 120°, V = 5626.7(3) Å^3, Z = 2, D_c = 1.614 g/cm^3, μ = 0.129 mm^{-1}, F(000) = 2766, crystal 0.33 × 0.13 × 0.11 mm^3, Θ_{max} = 23.24°, ranges −23 ≤ h ≤ 23, −23 ≤ k ≤ 23, −16 ≤ l ≤ 16, reflections collected = 50235, independent reflections = 5392, data/restraints/parameters 5392/2925/1368.

The distribution of intensities ($E^2 - 1$ = 0.939) and systematic absent reflections indicated two possible space groups; $P\bar{3}$ and $P3$. The space group $P\bar{3}$ was later determined to be correct. Direct methods of phase determination followed by two Fourier cycles of refinement led to an electron density map from which most of the non-hydrogen atoms were identified in the asymmetry unit of the unit cell. With subsequent isotropic refinement, all of the non-hydrogen atoms were identified. There were half a disordered-molecule of $C_{44}H_{10}F_{20}N_4$, one-third disordered-molecule of C_{60}, and two disordered solvent molecules of C_7H_8 present in the asymmetric unit of the unit cell. The C_{60} was refined where the 3-fold rotation special position was suppressed and with $^1/_3$ site occupancy. The $C_{44}H_{10}F_{20}N_4$ was located at the inversion center. The two $-C_6F_5$ groups were disordered (disordered site occupancy ratios were 77%/23% and 91%/9%). The H atom on the −NH group was refined as disordered positions between the two N-atoms (site occupancy ratio was 56%/44%). The two disordered C_7H_8 site occupancy ratios were 32%/40%/28% and 64%/36%. The H_2TPFPP/C_{60} unit cell ratio was 3:2.

Atomic coordinates, isotropic and anisotropic displacement parameters of all the non-hydrogen atoms were refined by means of a full matrix least-squares procedure on F^2. The H-atoms were included in the refinement in calculated positions riding on the atoms to which they were attached. The refinement converged at R1 = 0.0611, wR2 = 0.1694, with intensity $I > 2\sigma(I)$.

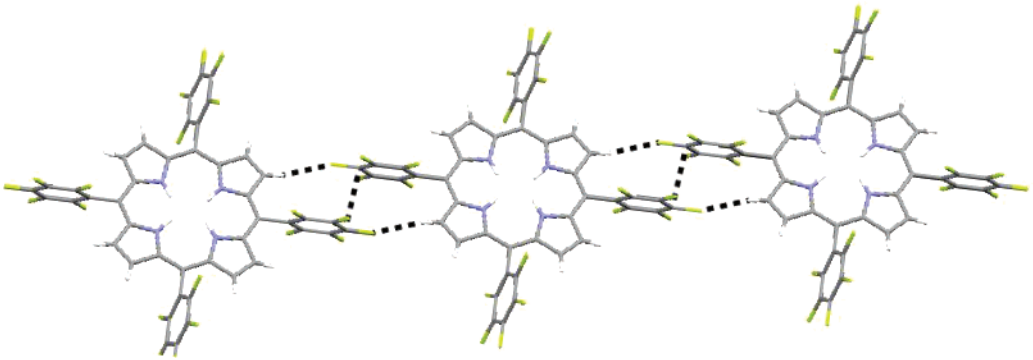

Figure 8. Formation of porphyrin tapes through *p*-phenyl C−F···H−C interactions between porphyrins from adjacent columns in H_2TPFPP·3*p*-Xylene, **2**.

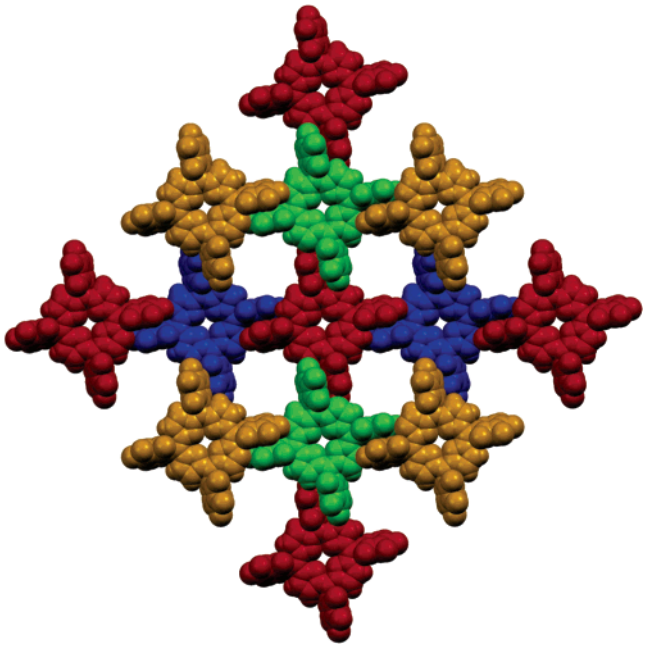

Figure 9. Porphyrin 3D network in H_2TPFPP·C_{60}·8Benzene, **3**. Arrangements relative to a plane of red porphyrins are as follows: blue, above; green, below. The yellow porphyrins lie below the plane of the green.

Results and Discussion

Equimolar solutions of tetrarylporphyrins and fullerenes often cocrystallize in a 1:1 ratio.[1] This persists when the porphyrin is tetra(pentafluorophenyl)porphyrin (H_2TPFPP) but there are differences and subtleties, depending on the crystallizing solvent. From *p*-xylene, crystals of an unsolvated 1:1 complex with C_{60} (**1**) are obtained, but crystals of fullerene-free *p*-xylene-solvated porphyrin (**2**) are also formed in the same mother liquor. From benzene, crystals of a benzene-solvated 1:1 complex with C_{60} (**3**) are formed. From toluene, crystals with a complex 3:2:6 stoichiometry of porphyrin/fullerene/solvent are preferred (**4**).

The recent report of Olmstead and Nurco[12] on the cocrystallization of free-base and nickel tetra(pentafluorophenyl)-porphyrins with fullerenes provides some interesting contrasts with the crystals presented here. Crystals grown in benzene from identical components by layering solutions rather than by slow evaporation are trigonal with a stoichiometry 3:2:6 ratio of H_2TPFPP/C_{60}/benzene[12] rather than 1:1:8 as found in **3**. The space group ($P\bar{3}$) and structure of this material is actually identical to that of **4** with toluene solvate molecules replaced by benzene. On the other hand, a structure identical to **3** with 1:1:8 stoichiometry is formed from layered benzene solutions of Ni(TPFPPP) with C_{60}.[12] It is apparent that the different crystallization procedures control the structural type produced. For the cocrystallates **3** and **4**, visual examination of the crystallized material suggests only one crystal type is formed with evaporative methods.

H_2TPFPP·C_{60}, 1. Porphyrin Sheets. Figure 1 shows the familiar porphyrin/fullerene supramolecular embrace in an alternating linear stack. The fullerene closely approaches the porphyrin with closest C to mean 24-atom plane distances of 2.65 and 2.71 Å. These distances lie at the short end of the range of observed distances,[1] indicating that the electron withdrawing effect of the pentafluorophenyl substituents on the porphyrin does little if anything to diminish the strength of the $\pi-\pi$ interaction. This is consistent with the understanding that although charge transfer may play a role in the fullerene/porphyrin interaction, it is minor compared to the $\pi-\pi$ bonding. The fullerene is precisely centered over the porphyrin with the 6:6 ring juncture "double" bonds closest. The 6:6 bond approach is more common than the 6:5 consistent with maximization of electron density in the $\pi-\pi$ interaction. The porphyrins are in strict tetragonal register along the crystallographic 4-fold axis as expected if the porphyrin/fullerene interaction is a major organizing structural element. This requires a 2-fold disorder in C_{60}, which is observed.

As shown in Figure 2, *ortho*-F atoms of the porphyrin are directed toward the centers of fullerene six-membered rings at F to nearest C atom distances of 3.17−3.76 Å. The distances of these F atoms to the centers of the fullerene six-membered rings are 2.94 and 3.22 Å for the two sets of four equivalent rings. The abundance and directionality of intermolecular C−F···π interactions in the Cambridge Database, greater than for the heavier halogens,[21] is taken as an indication that the interaction is attractive. The present F···C distances are toward the long end of the range (2.9−3.3 Å) indicating either that the interaction is relatively weak or that the van der Waals radius of a fullerene carbon atom is somewhat larger than in a regular, flat arene.

As shown in Figure 3, the porphyrins form a tetragonal sheet structure via novel C−F···H−C interactions from the *para*-F positions to neighboring pyrrole H atoms with fullerenes embedded within each sheet. As shown is Figure 4, these interactions occur in pairs with each pentafluorophenyl group, at F···H distances of 2.49 Å and nearly linear F···H−C angles (162°). The sum of the fluorine/hydrogen van der Waals radii is taken as 2.67 Å placing the present metrics at the shorter end of the range.[11] In addition to this end-to-end bond interaction, the *p*-C−F bond dipoles are aligned in antiparallel fashion at C···F separations of 3.41 Å. Both these interactions

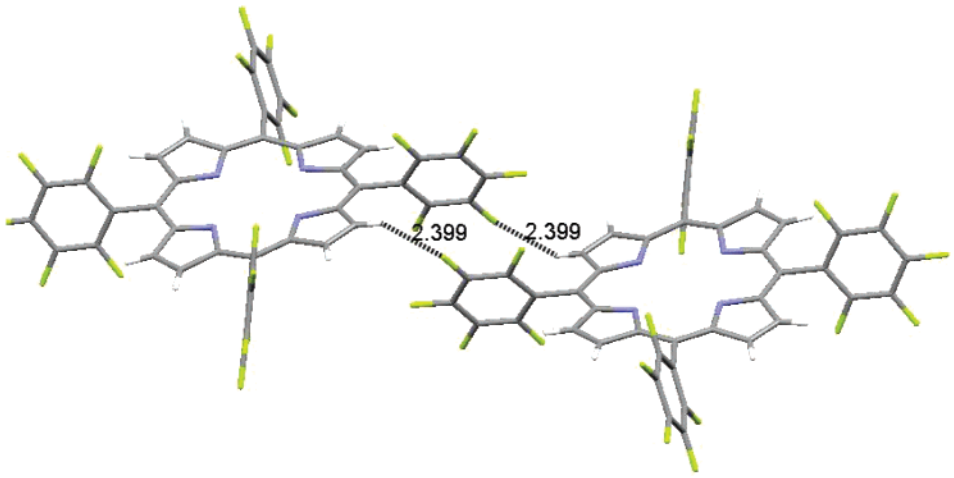

Figure 10. Detail of the *m*-phenyl C−F···H−C interactions between adjacent porphyrins in H_2TPFPP·C_{60}·8Benzene, **3**, that lead to the 3D arrangement in Figure 9.

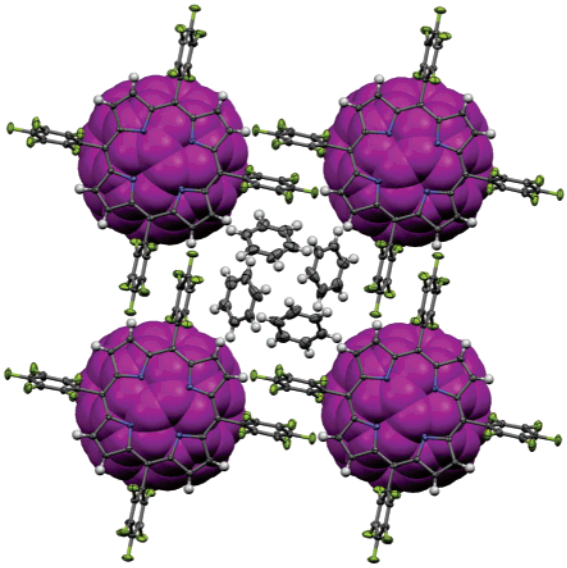

Figure 11. View down alternating columns of H_2TPFPP and C_{60} in H_2TPFPP·C_{60}·8Benzene, **3**, showing channels between columns occupied by benzene molecules with space-filling model for disordered C_{60} (one 50% site shown) and thermal ellipsoids (50% probability) for H_2TPFPP and benzene molecules.

are considered attractive and structure-defining. We have also observed that the *meta*-C−F bonds lie over neighboring pentafluorophenyl groups at F···F distance of 2.87 Å. The nominal F···F van der Waals separation is 2.94 Å so this approach might be also considered as an attractive interaction, but is more likely repulsive and the result of general packing effects.

To complete the description of the lattice structure of **1**, two identical sets of tetragonally stacked porphyrin layers with fullerene pillars interpenetrate. The result is the alternating layered sheet structure shown in Figure 5. The porphyrin layer to layer separation is 12.26 Å.

An analysis of the packing environment around each fullerene identifies, in addition to the C−F···π interactions discussed earlier, the close contacts shown in Figure 6. Contact *e* shows a pyrrole C−H bond approaching the electron rich 6:6 ring juncture at H···C distance of 2.87 Å. Contact *b* brings a *p*-F atom within 3.03 Å of a fullerene C atom. Both *e* and *b* are shorter than the sum of the van der Waals radii. Contacts *c*, *d*, and *e* are $\pi-\pi$ interactions between a fluoroarene and a fullerene with C···C separations of 3.04−3.14 Å. Fluoroarene/arene $\pi-\pi$ interactions are considered attractive in the range 3.4−3.8 Å suggesting that the closer approach with a fullerene is also attractive.

H_2TPFPP·3*p*-Xylene, 2. Porphyrin Tapes. This nonfullerene containing structure provides an opportunity to independently assess fluoroporphyrin/fluoroporphyrin interactions. As expected from the tetraarylporphyrin work of Strouse,[22] occlusion of lattice solvent molecules is observed. As shown in Figure 7, one disordered *p*-xylene solvate molecule is found sandwiched between porphyrin stacks. The other disordered *p*-xylene fills space between these stacks and shares in a number of contacts with the porphyrins at close to van der Waals distances.

Notably, the fluoroporphyrins in **2** have the same pairwise phenyl C−F to pyrrole H−C interactions observed in **1**. However, only half of the pentafluorophenyl groups participate, so the structure of **2** has tapes of porphyrins rather than sheets. This is illustrated in Figure 8 which also shows close *p*-C··· *p*-F approaches at 3.39 Å. The dimensions in the C−F···H−C interactions in **2** (F···H = 2.55 Å, F···H−C angle = 152°) indicate a slightly weaker interaction compared with **1** but are otherwise very similar. The occurrence of fluorophenyl/pyrrole interactions in both **1** and **2** attests to its importance as a structure-defining element.

H_2TPFPP·C_{60}·8Benzene, 3. Porphyrin 3D Network. When the 1:1 complex of C_{60} and H_2TPFPP is formed in benzene rather than *p*-xylene, the pentafluorophenyl/pyrrole interaction observed in **1** and **2** switches to the *meta* rather than the *para* C−F bond. As shown in Figure 9, this enables the porphyrins to propagate in three dimensions. Stepped tape and sheet motifs can still be discerned. The details of the C−F···H−C interactions are illustrated in Figure 10. The *meta* contact in **3** (2.40 Å) is closer than the *para* contacts in **1** and **2** but the F···H−C angle (135°) is much farther removed from linearity. As shown in Figure 11, the expected linear stacks of alternating porphyrins and fullerenes are observed in this structure and the spaces between the columns are filled with ordered benzene molecules. Typical C−H to π−benzene interactions can be observed from both pyrrole and benzene C−H groups.

3H_2TPFPP·2C_{60}·6Toluene, 4. Porphyrin Tapes and Prisms. A 1:1 complex of C_{60} and H_2TPFPP is not formed when the crystallization solvent is toluene. Rather, the stoichiometry is three porphyrins to two fullerenes. The structure is complex but can be described in terms of trigonal prismatic arrangements of porphyrin tape motifs. The tapes are formed via *meta*-C−F

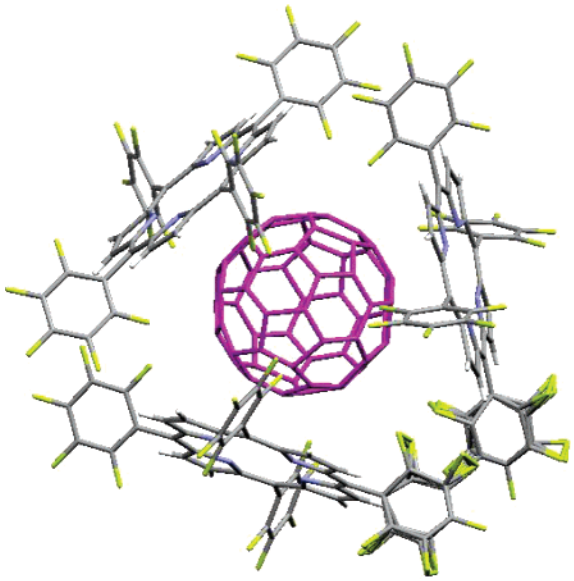

Figure 12. Prismatic arrangement of three H_2TPFPP molecules around a C_{60} from adjacent porphyrin tapes in $3H_2TPFPP{\cdot}2C_{60}{\cdot}6$Toluene, **4**.

to pyrrole H−C bonding closely related to that observed in **3** (Figure 10). The dimensions of the bridge (F···H = 2.46 Å, ∠F···H−C = 127°) indicate that the interaction is weaker than in **3**. As shown in Figure 12, three of these tapes are arranged in a manner that creates a trigonal prismatic cup for complexation of C_{60}. The C_{60} is rotationally disordered. Interestingly, the same *meta*-C−F to pyrrole H−C interactions are responsible for positioning the tapes in this prismatic array. The complexation of a fullerene by *three* porphyrins, rather than two, has not been observed before. The C−F···H−$C_{pyrrole}$ interactions lock the porphyrins into a somewhat closer approach to each other than observed in earlier structures using tetraphenyl- or octaethyl-porphyins. It suggests a new target for a tri-porphyrin supramolecular host for fullerenes. Cyclic[23] and acyclic ("Jaws") bis-porphyrins[24] are currently used to complex fullerenes in solution. Despite tri-porphyrin complexation of C_{60}, the familiar zigzag alternation of fullerenes and porphyrins seen in most tetraarylporphyrin structures can be observed in **4**. This is illustrated in the bottom half of Figure 13. There are close approaches of one mean 24 atom porphyrin plane to the 6:6 ring (2.78, 2.86 Å) and of 6:5 ring junctions to the other two porphyrins (2.78, 2.89, 2.88, 2.99 Å). There are cavities at the center of the hexagon of prisms in Figure 13 which contain 6 toluene solvates held in place by typical arene/fluoroarene $\pi-\pi$ stacking with H···F distances of 3.23 Å and C···C distances of 3.58 Å. To make up the complete structure, the molecules projected onto Figure 13 in a 2D honeycomb are repeated along the perpendicular 3-fold axes such that the inter-fullerene spacing is quite large (> 7.7 Å).

Conclusion

A new intermolecular crystal interaction involving pairs of C−F···H−C interactions from pentafluorophenyl groups and porphyrinic pyrroles has been recognized (Figures 4, 10). It is common to all four structures crystallized from 1:1 fullerene/porphyrin cocrystallization attempts using tetra(pentafluorophenyl)porphyrin, indicating that it is a structure-defining element. It is manifest in tape or tape-like linking of the tetra(pentafluorophenyl)porphyrins that support the fullerene/porphyrin $\pi-\pi$ attraction. This interaction is present in varying degrees in all but one of the seventeen structures involving tetra-

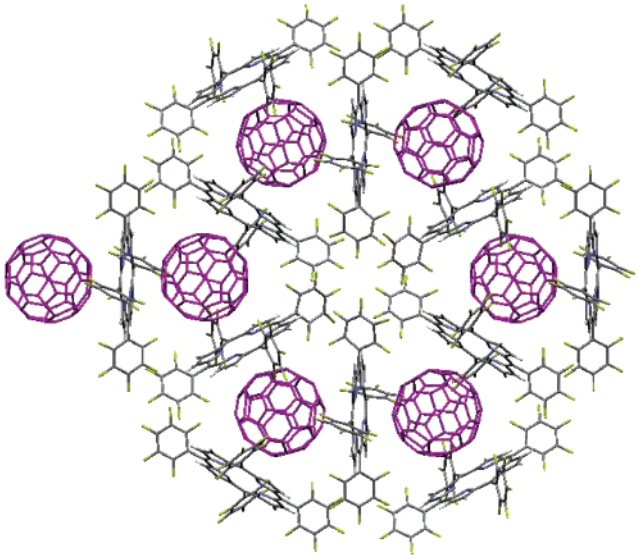

Figure 13. View perpendicular to the crystallographic 3-fold axis showing the 2-D honeycomb arrangement of fullerenes and porphyrins.

(pentafluorophenyl)porphyrin that are found in the Cambridge Crystallographic Data Base but it had not been recognized previously. It allows porphyrins to more closely approach each other than in nonfluorinated tetrarylporphyrins, allowing C_{60} to simultaneously interact with three rather than two porphyrins. In view of the paradigm of supramolecular chemistry whereby a portion of a crystal structure is used to design discrete molecular hosts for complementary guests, structure **4** suggests that trigonal prismatic tris-porphyrin hosts might have high binding constants for fullerenes.

Acknowledgment. This work was supported by the Marsden Fund of The Royal Society of New Zealand (Grant 00-UOA-015), The University of Auckland Research Committee, and the General Medical Institute of the National Institutes of Health (Grant GM 23851).

Supporting Information Available: X-ray crystallographic files in CIF format for compounds **1**−**4**. This information is available free of charge via the Internet at http://pubs.acs.org.

References

(1) Boyd, P. D. W.; Reed, C. A. *Acc. Chem. Res.* **2005**, *38*, 235−242.
(2) Boyd, P. D. W.; Hodgson, M. C.; Chaker, L.; Rickard, C. E. F.; Oliver, A. G.; Brothers, P. J.; Bolskar, R.; Tham, F. S.; Reed, C. A. *J. Am. Chem. Soc.* **1999**, *121*, 10487−10495.
(3) Olmstead, M. M.; Costa, D. A.; Maitra, K.; Noll, B. C.; Phillips, S. L.; Van Calcar, P. M.; Balch, A. L. *J. Am. Chem. Soc.* **1999**, *121*, 7090−7097.
(4) Sun, D.; Tham, F. S.; Reed, C. A.; Boyd, P. D. W. *Proc. Natl. Acad. Sci. U.S.A.* **2002**, *99*, 5088−5092 and references therein.
(5) Olmstead, M. M.; Lee, H. M.; Duchamp, J. C.; Stevenson, S.; Marciu, D.; Dorn, H. C.; Balch, A. L. *Angew. Chem., Int. Ed.* **2003**, *42*, 900−903 and references therein.
(6) Hochmuth, D. H.; Michel, S. L. J.; White, A. J. P.; Williams, D. J.; Barrett, A. G. M.; Hoffman, B. M. *Eur. J. Inorg. Chem.* **2000**, *4*, 593−596.
(7) Konarev, D. V.; Neretin, I. S.; Slovokhotov, Y. L.; Yudanova, E. I.; Drichko, N. V.; Shul'ga, Y. M.; Tarasov, B. P.; Gumanov, K. L.; Batsanov, A. S.; Howard, J. A. K.; Lyubovskaya, R. N. *Chem.—Eur. J.* **2001**, *7*, 2605−2616.
(8) Ishii, T.; Aizawa, N.; Kanehama, R.; Yamashita, M.; Sugiura, K. I.; Miyasaka, H. *Coord. Chem. Rev.* **2002**, *226*, 113−124.
(9) Wang, Y. B.; Lin, Z. Y. *J. Am. Chem. Soc.* **2003**, *125*, 6072−6073.
(10) Dunitz, J. D.; Taylor, R. *Chem.—Eur. J.* **1997**, *3*, 89−98.
(11) Reichenbacher, K.; Suss, H. I.; Hulliger, J. *Chem. Soc. Rev.* **2005**, *34*, 22−30.

(12) Olmstead, M. M.; Nurco, D. J. *Cryst. Growth Des*., published online Sept. 1, 2005, http://dx.doi.org/10.1021/cg050225r.
(13) Longo, F. R.; Finarelli, M. G.; Kim, J. B. *J. Heterocycl. Chem.* **1969**, *6*, 927−931.
(14) Sheldrick, G. M. *SADABS: Program for semiempirical absorption correction*; University of Göttingen: Germany, 1997.
(15) Parkin, S.; Moezzi, B.; Hope, H. *J. Appl. Crystallogr.* **1995**, *28*, 53−56.
(16) Farrugia, L. J. *J. Appl. Crystallogr.* **1999**, *32*, 837−838.
(17) Sheldrick, G. M. *SHELX97 [Includes SHELXS97, SHELXL97, CIFTAB] − Programs for Crystal Structure Analysis*, release 97-2; Institüt für Anorganische Chemie der Universität: Göttingen, Germany, 1997.
(18) Altomare, A.; Cascarano, G.; Giacovazzo, C.; Guagliardi, A. *J. Appl. Crystallogr.* **1993**, *26*, 343.
(19) *SHELXTL Bruker*, *6.14*; Bruker AXS Inc.: Madison, WI, 2003.
(20) Bruno, I. J.; Cole, J. C.; Edgington, P. R.; Kessler, M.; Macrae, C. F.; McCabe, P.; Pearson, J.; Taylor, R. *Acta Crystallogr.* **2002**, *58*, 389−397.
(21) Prasanna, M. D.; Row, T. N. G. *Cryst. Eng.* **2000**, *3*, 135−154.
(22) Byrn, M. P.; Curtis, C. J.; Hsiou, Y.; Khan, S. I.; Sawin, P. A.; Tendick, S. K.; Terzis, A.; Strouse, C. E. *J. Am. Chem. Soc.* **1993**, *115*, 9480−9497.
(23) Tashiro, K.; Aida, T.; Zheng, J.-Y.; Kinbara, K.; Saigo, K.; Sakamoto, S.; Yamaguchi, K. *J. Am. Chem. Soc.* **1999**, *121*, 9477−9478.
(24) Sun, D. Y.; Tham, F. S.; Reed, C. A.; Chaker, L.; Boyd, P. D. W. *J. Am. Chem. Soc.* **2002**, *124*, 6604−6612.

CG050352N